



Title	Swim bladder collagen forms hydrogel with macroscopic superstructure by diffusion induced fast gelation
Author(s)	Mredha, Md. Tariful Islam; Zhang, Xi; Nonoyama, Takayuki; Nakajima, Tasuku; Kurokawa, Takayuki; Takagid, Yasuaki; Gong, Jian Ping
Citation	Journal of materials chemistry b, 3(39), 7658-7666 <a href="https://doi.org/10.1039/c5tb00877h">https://doi.org/10.1039/c5tb00877h</a>
Issue Date	2015-10-21
Doc URL	<a href="http://hdl.handle.net/2115/63152">http://hdl.handle.net/2115/63152</a>
Type	article (author version)
File Information	Revised manuscript.pdf



[Instructions for use](#)

1 *Regular article*

2

3 **Swim bladder collagen forms hydrogel with macroscopic superstructure by**  
4 **diffusion induced fast gelation**

5

6

7 Md. Tariful Islam Mredha<sup>a</sup>, Xi Zhang<sup>b</sup>, Takayuki Nonoyama<sup>c</sup>, Tasuku Nakajima<sup>c</sup>, Takayuki  
8 Kurokawa<sup>c</sup>, Yasuaki Takagi<sup>d</sup> and Jian Ping Gong<sup>c\*</sup>

9

10 <sup>a</sup>*Graduate School of Life Science, Hokkaido University, Sapporo 060-0810, Japan*

11 <sup>b</sup>*Graduate School of Fisheries Sciences, Hokkaido University, Hakodate 041-8611, Japan*

12 <sup>c</sup>*Faculty of Advanced Life Science, Hokkaido University, Sapporo 060-0810, Japan*

13 <sup>d</sup>*Faculty of Fisheries Sciences, Hokkaido University, Hakodate 041-8611, Japan*

14

15

16

17

18

19

20

21

22 *\*Corresponding author*

23 *E-mail: gong@mail.sci.hokudai.ac.jp (J.P.G); Tel & FAX: +81-(0)11-706-2774*

24

25

26 **ABSTRACT:** Marine collagen has been attracting attention as medical materials in recent  
27 times due to the low risk of pathogen infection compared to animal collagen. Type I collagen  
28 extracted from swim bladder of Bester sturgeon fish has excellent characteristics such as high  
29 denaturation temperature, high solubility, low viscosity and extremely fast rate to form large  
30 bundle of fiber at certain conditions. These specific characteristics of swim bladder collagen  
31 (SBC) permit us to create stable, disk shaped hydrogels with concentric orientation of  
32 collagen fiber by the controlled diffusion of neutral buffer through collagen solution at room  
33 temperature. However, traditionally used animal collagens, e.g. calf skin collagen (CSC) and  
34 porcine skin collagen (PSC) could not form any stable and oriented structure by this method.  
35 The mechanism of superstructure formation of SBC by diffusion induced gelation process has  
36 been explored. The fast fibrillogenesis rate of SBC causes a quick squeezing out of solvent  
37 from the gel phase to the sol phase during gelation, which builds an internal stress at the gel-  
38 sol interface. The tensile stress induces the collagen molecules of gel phase to align along the  
39 gel-sol interface direction to give this concentric ring-shaped orientation pattern. On the other  
40 hand, the slow fibrillogenesis rate of animal collagens due to the high viscosity of the  
41 solution does not favor the ordered structure formation. The denaturation temperature of SBC  
42 increases significantly from 31°C to 43°C after gelation, whereas that of CSC and PSC was  
43 found to increase a little. Rheology experiment shows that SBC gel has storage modulus  
44 larger than 15 kPa. The SBC hydrogels with thermal and mechanical stability have potentials  
45 as bio-materials for tissue engineering applications.

46

47

48 *Key words:* Hydrogel, swim bladder collagen, superstructure, diffusion, denaturation  
49 temperature.

50

## 51 1. INTRODUCTION

52 Hydrogels, a class of soft and wet material, are considered to be the most promising smart  
53 bio-materials due to their similarity to soft bio-tissues. Developments of hydrogels in last  
54 decade<sup>1-5</sup> greatly enhanced the applications of this material in various fields, including  
55 artificial organs, drug delivery, regenerative medicine etc.<sup>6-9</sup> Collagen-based hydrogels for  
56 biomedical application are becoming very hot topic in medical research because of their low  
57 antigenic activity, high cell adhesion properties, biocompatibility, and biodegradability.<sup>10,11</sup>  
58 Numerous specific functions of many bio-tissues are strongly dependent on the anisotropic  
59 superstructure of fiber-forming collagen.<sup>12,13</sup> The most common sources of collagen for  
60 biomaterials and tissue engineering are bovine skin and tendons, porcine skin, and rat tail.<sup>11</sup>  
61 In recent times, the use of collagen and collagen-derived products from land-based animal  
62 calls into question because of the emergence of zoonosis such as bovine spongiform  
63 encephalopathy (BSE), foot-and-mouth disease (FMD), avian influenza diseases etc.<sup>14,15</sup>  
64 Religious beliefs also restrict the usage of porcine or bovine collagens. Marine resource has  
65 been attracting attention at the very recent times as a smart alternative of animal collagen due  
66 to their low risk of pathogen infection and no religious obstruction.<sup>16</sup>

67

68 A huge source of marine-based collagen is now from the wastes of seafood industry.  
69 Recently, Zhang *et al.*<sup>17</sup> have found that the swim bladder of Bester sturgeon fish (a hybrid  
70 sturgeon of *Husohuso* x *Acipenserruthenus*) is a large source of type I collagen (18.1% on a  
71 wet weight basis, 37.7% on a dry weight basis), which has relatively high thermal stability  
72 (32.9°C by CD spectroscopy). In addition, apart from the conventional animal collagen, this  
73 swim bladder collagen (SBC) has excellent characteristics such as high solubility and  
74 homogeneity, low viscosity and extremely fast rate to form large bundle of fiber at certain  
75 conditions. However, collagens from other tissues (scales, skin, muscle, digestive tract,

76 notochord and snout cartilage) of Bester sturgeon do not show those interesting properties.<sup>17</sup>  
77 Until now, hydrogels from marine-based collagen have hardly been developed because of the  
78 poor availability in comparison with the land-based animal collagen that is abundant in the  
79 market.<sup>18,19</sup> Being a marine sourced atelocollagen, SBC is expected to have low antigenicity  
80 with less risk of pathogen infection and thus, would be suitable for medical application.<sup>16</sup>  
81 However, the immunostimulant characteristics may not always depend only on the terminal  
82 group, the removal of telopeptide group would be preferable to make a biomaterial with  
83 relatively better safety profile.<sup>20,21</sup> In this work, we focus on developing collagen hydrogels  
84 with ordered structure by utilizing this marine sourced type I atelocollagen that has the  
85 distinguished properties.

86

87 Many efforts have been made for creating ordered structure in collagen-based materials by  
88 various methods, including dialysis, shear, hydrodynamic flow, electric field, electro-  
89 spinning and magnetic field techniques.<sup>22-29</sup> In this work, we use the diffusion-induced  
90 gelation to prepare SBC hydrogels. It is well-known that negatively charged polyelectrolytes  
91 having rigid nature, such as DNA, alginate, and poly(2,2'-disulfonyl-4,4'-benzidine  
92 terephthalamide) (PBDT) form physical hydrogels when  $\text{Ca}^{2+}$  ions are allowed to diffuse into  
93 these polymer solutions.<sup>30-37</sup> Furthermore, these rigid molecules after gelation are orientated  
94 perpendicular to the diffusion direction of  $\text{Ca}^{2+}$  ion.<sup>34-37</sup> This specific superstructure formation  
95 during diffusion-induced gelation has been related to the syneresis effect of gelation.<sup>37</sup> That is,  
96 the complexation of negatively charged rigid macromolecules with  $\text{Ca}^{2+}$  leads to gelation,  
97 which induces shrinkage of the gel phase. Since the sol phase does not shrink, an internal  
98 stress is built at the sol-gel interface, where the sol phase exerts a tension to the gel phase and  
99 the gel phase exerts a compression to the sol phase. As a result, the macromolecules in the gel  
100 phase orient along the tensile direction. Our previous study also revealed that, when we

101 develop programmed swelling mismatch in different regions of a hydrogel containing semi-  
102 rigid macromolecules, the mismatch induced internal stress determine the orientation of  
103 macromolecules in respective regions.<sup>5</sup>

104

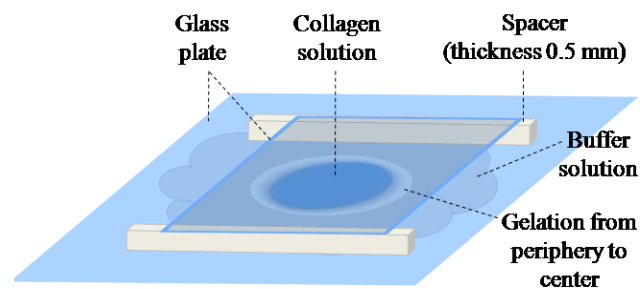
105 Although different rigid macromolecules are successfully oriented by diffusion induced  
106 gelation process, but still now, it remains a challenge to make oriented structure in collagen  
107 hydrogel due to some limitations of animal collagen. In this work, we intend to develop  
108 collagen hydrogels with ordered structure based on this mechanism by utilizing the  
109 distinguished properties of SBC. Previous study has clarified that SBC molecules are in  
110 stable triple-helix molecular form in acidic solution, and they self-assemble into fibrils in  
111 neutral buffer.<sup>17</sup> This is because in acidic solution the collagen is positively charged and in  
112 the neutral buffer, it becomes almost neutral, which favors fibril formation.<sup>38,39</sup> Thus, if we  
113 perform controlled diffusion of neutral buffer into acidic SBC solution, we expect super  
114 structure formation of SBC molecule by quick fibrillogenesis of the rigid SBC molecule.

115

## 116 **2. EXPERIMENTAL SECTION**

117 **Materials:** Type I collagen (atelocollagen) was extracted from the swim bladder of Bester  
118 sturgeon fish according to the previously reported protocol.<sup>17</sup> The swim bladder collagen was  
119 denoted as SBC. Type I calf skin collagen, CSC (tropocollagen, Sigma Aldrich, Japan) and  
120 Type I porcine skin collagen, PSC (atelocollagen, Nippi Co. Ltd.) were used as received  
121 without further purifications. Analytical grade  $\text{Na}_2\text{HPO}_4$  and  $\text{NaH}_2\text{PO}_4$  (Wako Pure Chemical  
122 Industries Ltd., Japan) were used as received for the preparations of Na-phosphate buffer  
123 solution of pH 7.2. Concentrated HCl (Wako Pure Chemical Industries Ltd., Japan) was used  
124 to prepare aqueous HCl solution of pH 2.5 for the preparation of collagen solutions. All the  
125 aqueous solutions were prepared using ultrapure deionized water.

126 **Diffusion induced gelation process:** To prepare collagen solution, a prescribed amount of  
127 collagen was dissolved in *aq.* HCl (pH 2.5). The mixture was left for 3 days without any  
128 external perturbations at room temperature (25°C) to get a homogenous solution. After that, a  
129 drop (~20 μL) of collagen solution was placed on a glass plate and covered by another glass  
130 plate with a gap distance of 0.5 mm, which was controlled by two silicone spacer, as shown  
131 in Figure 1. The disk-shaped collagen solution was in contact with the glass plates with an  
132 initial diameter about ~6 mm. Gelation of collagen was performed by introducing 0.1 M Na-  
133 phosphate buffer (pH 7.2) into the reaction cell from the peripheral part of collagen solution.  
134 Gelation progressed from periphery to center of the collagen solution by the diffusion of  
135 buffer. After 2 hours, disk shaped collagen hydrogel with diameter ~6 mm and thickness 0.5  
136 mm was formed. For rheological study, we have prepared collagen gel of thickness 1 mm. All  
137 the SBC gels were prepared at room temperature (25°C). However; CSC and PSC gels were  
138 prepared at 25°C and 34°C. To prepare CSC and PSC gels at 34°C, the collagen and buffer  
139 solutions were pre-incubated at that temperature for 10 minutes before starting gelation.



140  
141 **Figure 1** Set up for the diffusion induced gelation process of collagen solution. The diameter  
142 of the disc-shaped collagen solution was about 6 mm.

### 143 **Characterization:**

#### 144 **Structure**

145 Time dependent structural change during gelation was monitored under the polarizing optical  
146 microscope, POM (Nikon, LV100POL). A color sensitized 530 nm tint plate was used to  
147 distinguish collagen orientation. The birefringence at different regions of hydrogel was

148 measured quantitatively from the retardation values using a Berek compensator in POM.  
149 Scanning electron microscopy (SEM) (JSM-6010LA, JEOL Ltd.) was applied to study the  
150 morphology and orientation of collagen fibril. To prepare the sample for SEM observation,  
151 the samples were fixed by 0.1 % (v/v) *aq.* glutaraldehyde for 24 hours and freeze-dried using  
152 a freeze drying device (Advantage XL-70, VirTis freeze-dryer) and finally, coated with gold  
153 using an ion-sputtering device (E-1010, Hitachi, Japan). The shape of the sample did not  
154 change after freeze drying.

### 155 **Fibrillogenesis**

156 Fibrillogenesis rate of collagen was studied by monitoring the turbidity change of an equal  
157 volume mixture of 0.3 wt % collagen and 0.1 M Na-phosphate buffer (pH 7.2) at 320 nm  
158 using a quartz cell of 1 cm path length in UV spectrophotometer (UV-1800, Shimadzu UV  
159 Spectrophotometer).

### 160 **Solution properties**

161 Transparency of collagen solution was determined from the turbidity measurement at 320  
162 nm. The dynamic viscosity of collagen solution was measured at 25°C using rheometer  
163 (ARES-100FRT) by strain controlled steady rate sweep test with a cone and plate geometry  
164 of 25 mm diameter, 0.054 mm gap distance and 0.04 radians cone angle, covering a shear rate  
165 ranges from 0.1 s<sup>-1</sup> to 10 s<sup>-1</sup>.

### 166 **Thermal stability**

167 The denaturation temperature of collagen solution and collagen hydrogel was determined by  
168 differential scanning calorimetry, DSC (SII X-DSC7000, SII Nanotechnology Inc.).

### 169 **Mechanical property**

170 To study the mechanical strength of SBC hydrogel, a dynamic frequency sweep test was  
171 performed from 0.25 s<sup>-1</sup> to 100 s<sup>-1</sup> with a shear strain of 0.2 % in the parallel plate geometry

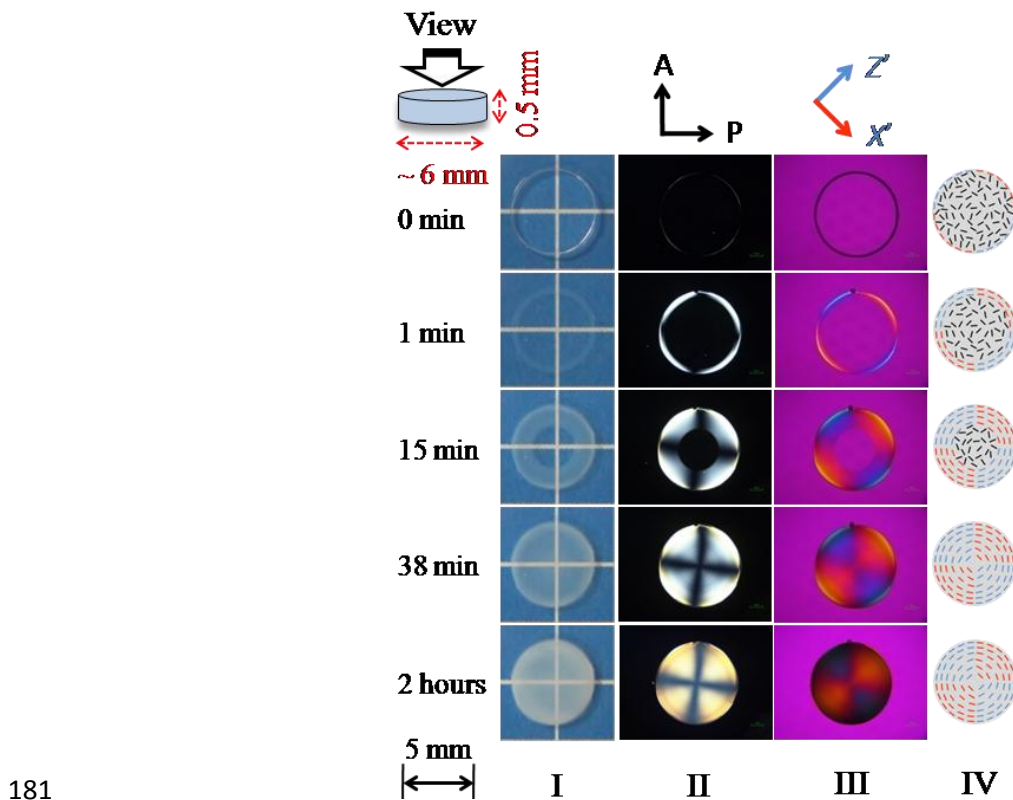


172 at 25°C. A disk shaped SBC gel of thickness 1 mm and diameter 6 mm was adhered to the  
 173 plates using glue for measurement.

174

175 **3. RESULTS AND DISCUSSION**

176 When 0.1 M Na-phosphate buffer solution (pH 7.2) was introduced into the periphery of 4  
 177 wt% SBC solution, gelation started immediately from the peripheral part of collagen solution,  
 178 which could be confirmed from the turbidity appearance as shown in Figure 2(I). Gelation  
 179 continued to progress from the outside to the inside as the buffer solution slowly diffused into  
 180 the collagen solution.



181

182 **Figure 2** (I) Photographic images of 4 wt% SBC hydrogel at different gelation time. (II, III)  
 183 POM images under crossed polarizer in absence (II) and presence (III) of color sensitized 530  
 184 nm tint plate. All the images are in same scale as shown in the bottom left part. (IV)  
 185 Illustrations of orientation structure of SBC identified by POM. A: analyzer, P: polarizer. X'  
 186 and Z': fast and slow axes of tint plate, respectively.

187 To confirm the presence of oriented structure, we observed the time lapse of gelation  
188 processes under POM using crossed polarizer (Figure 2(II)). Before the addition of buffer, no  
189 birefringence was observed except at the periphery of collagen solution, indicating that the 4  
190 wt% SBC solution is isotropic, well below the liquid crystalline (LC) concentration. This is in  
191 consistent with the result by M.M. Giraud-Guille *et al.*,<sup>40-41</sup> who found that the LC phase of  
192 the type I rat tail collagen appears at critical concentration of 8~8.5 wt% in 0.5 M acetic acid  
193 (pH 2.5). The peripheral circular birefringence is considered as the edge effect of  
194 concentrated polymer solution. The collagen molecules of rigid triple helix assembled at the  
195 edge of liquid-air interface to show this ring shaped thin birefringence.

196

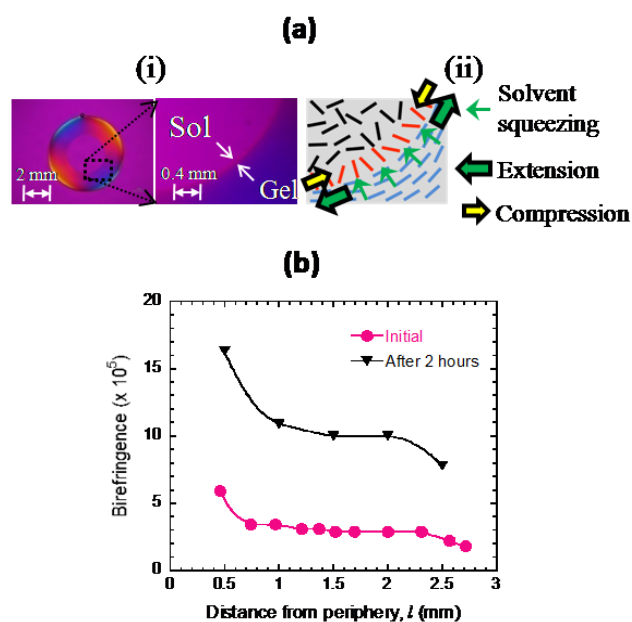
197 The cross patterned of strong birefringence were observed as the gelation progressed from the  
198 periphery to center (Figure 2(II)), which indicates the formation of radially or concentrically  
199 oriented structure during the diffusion induced gelation process. To confirm the orientation  
200 direction, we used color sensitized 530 nm tint plate during POM observation. Denoting that  
201 collagen has a positive birefringence<sup>42</sup>, the alternative ring shaped blue (quadrants 2 and 4)  
202 and orange (quadrants 1 and 3) colors in POM images (Figure 2(III)) indicate that the  
203 collagen molecules orient along and perpendicular to the tint polymer direction, respectively.  
204 That is, the collagen is oriented concentrically in the birefringence ring (Figure 2(IV)), in  
205 similar to previously reported results on other rigid molecules.<sup>37</sup> When the gelation reached  
206 the center of the sample at 38 minutes, the concentric orientation was developed in the whole  
207 sample. Rigid triple helix collagen molecules have positive charges at acidic condition.<sup>38</sup>  
208 Once the collagen molecules meet with the neutral buffer at the diffusion front, they form  
209 aggregated fibers by neutralization. The *syneresis* effect during fiber formation process is  
210 considered to be responsible for this super structure formation, in similar to previously  
211 reported mechanism.<sup>5</sup> The fibrillogenesis process causes solvent transportation

212 microscopically, and thus a swelling mismatch is built at the sol/gel interface which insists  
213 ordered structure formation. It should be mentioned that the volume change of the gel by  
214 contraction during gelation is difficult to observe at macroscopic scale. This is probably due  
215 to relatively strong adhesion of the collagen gel to the glass wall of the reaction chamber,  
216 which prevents the overall volume change of the gel.

217

218 The *syneresis* induced swelling mismatch can be justified when we observe the gelation front  
219 line *in situ* very carefully. A thin line of orange color (indicated by white arrow) ahead of the  
220 blue color can be identified at the diffusion front of sol-gel interface (Figure 3(a)(i)). This  
221 indicates the presence of radial orientation of collagen ahead of the gelation front as  
222 illustrated in Figure 3(a)(ii), which gradually converted into concentric orientation and  
223 stabilized with time by forming fiber. During fibrillogenesis process, the contracting gel  
224 phase experiences a tensile stress from the very adjacent sol phase. Oppositely, sol phase  
225 experiences a compressive stress from the contracting gel phase. Those opposite forces create  
226 the concentric and radial orientation in the gel phase and sol-gel boundary, respectively  
227 (Figure 3(a)(ii)).

228



229

230 **Figure 3 (a)** POM image (i) of the diffusion/gelation front region under magnified lens and  
 231 the corresponding schematic representation (ii) of orientation structure of SBC identified by  
 232 POM. **(b)** The birefringence of 4 wt% SBC gel at the position right behind the advancing  
 233 gelation front which corresponds to the initially formed structure (denoted as initial in the  
 234 Figure) and after 2 hours gelation vs. distance from periphery to center,  $l$ .

235

236 The birefringence increases with time. The initial birefringence right behind the gelation front,  
 237 which means the structure newly formed with the progress of the diffusion front, is shown in  
 238 Figure 3(b). The birefringence obtained after 2 hours gelation is about ~3 times higher than  
 239 the initial birefringence. The turbidity of the gel also increases drastically during this process  
 240 (Figure 2(I)). This observation suggests that fibrillogenesis process continues for the longer  
 241 period of time until they reach their characteristic fiber size.

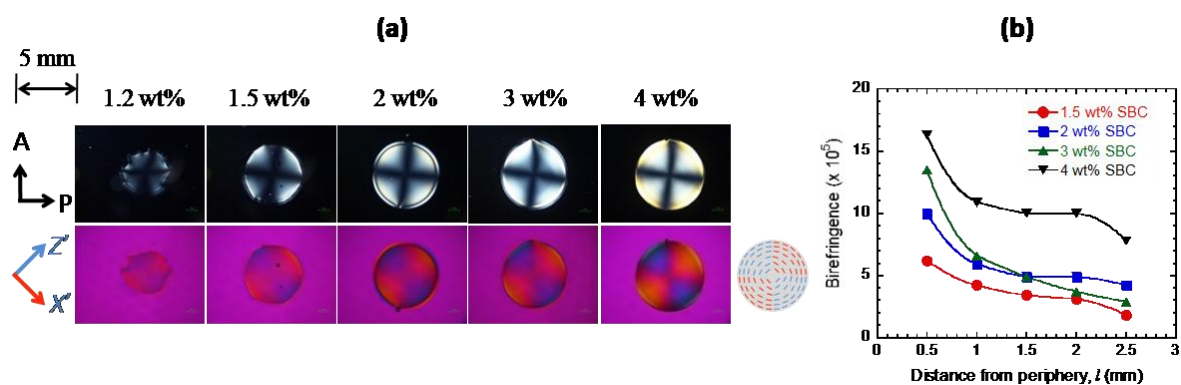
242

243 To understand the effect of collagen concentration on superstructure formation, we have  
 244 prepared hydrogel from low to high concentrations of SBC (1.2 ~ 4 wt%). At 1.2 wt% SBC,  
 245 the hydrogel only showed weak and irregular birefringence (Figure 4(a)). From 1.5 wt%,

246 distinct cross-patterns were observed, indicating the formation of concentric structure.  
247 Therefore, the minimum concentration of SBC required to form a well oriented gel is around  
248 1.5 wt%. In addition, at 1.5 wt%~3 wt%, but not at 4 wt%, a thin radially oriented layer can  
249 be noticed at the peripheral region (at the boundary of the gel and the buffer). As the viscosity  
250 of 1.5 ~ 3 wt% is lower than 4 wt%, this may make it possible for a little outflow of collagen  
251 solution at the periphery by the strong diffusion of buffer, which creates this radial  
252 orientation at the outer part of hydrogel.

253

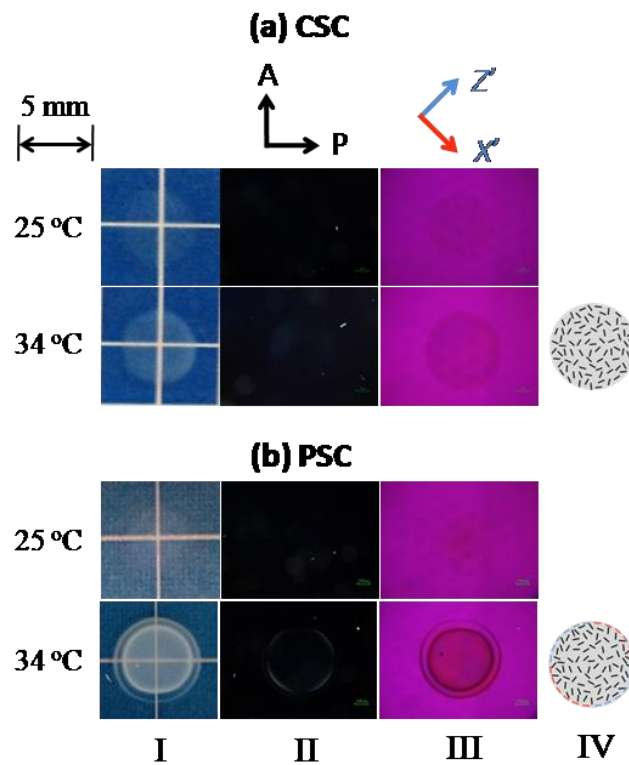
254 It could be observed from Figure 4(a) that the birefringence brightness changes with the  
255 concentrations of SBC. The brightness of periphery of hydrogel is stronger than that of the  
256 center. The birefringence variation with the distance from periphery to center ( $l$ ) of SBC  
257 hydrogels of various concentrations is shown in Figure 4(b). For all the concentrations of  
258 SBC, the birefringence decreases with  $l$ , which indicates that a gradient of orientation degree  
259 is created by the diffusion induced gelation process. Up to ~1 mm distance, birefringence  
260 decreases sharply. This is because that the diffusion velocity of buffer sharply decreases at  
261 the beginning as the gel width increases and therefore, the rate of fibrillogenesis also  
262 decreases. So the swelling mismatch created from *syneresis effect* also decreases which  
263 generates low internal tensile stress in the gel phase. Hence the orientation degree decreases.  
264 However, at the end (close to the center of the gel), birefringence decreases sharply. We  
265 considered that at the central part of the gel, the collagen molecules are subjected to tensile  
266 stress from all directions, which leads to the formation of poorly oriented structure.



267  
 268 **Figure 4 (a)** POM images (crossed polarizer both in absence and presence of tint plate) of  
 269 SBC hydrogels (1 hour gelation) prepared at 25°C having concentration ranges from 1.2 wt%  
 270 to 4 wt%. Illustration of orientation structure of SBC identified by POM is shown on the right  
 271 side of POM images. A: analyzer, P: polarizer, X' and Z': fast and slow axes of the tint plate,  
 272 respectively. All the POM images are in same scale as shown in the top left part. **(b)** The  
 273 birefringence variation of SBC hydrogel (2 hours gelation), with the distance from periphery  
 274 to center ( $l$ ) of the hydrogel.

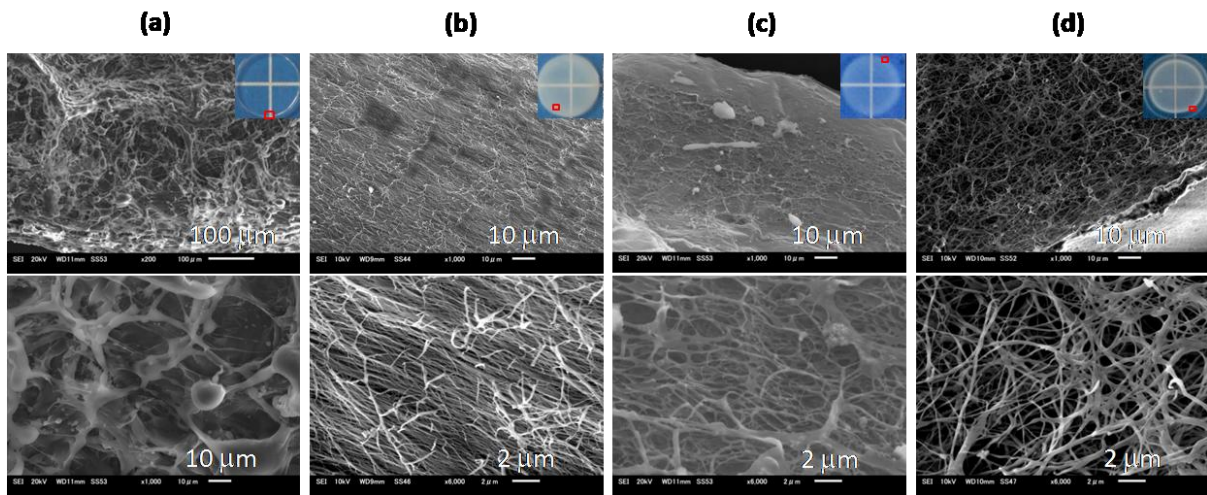
275  
 276 Diffusion induced superstructure formation in SBC hydrogel is quite similar to our previous  
 277 study,<sup>37</sup> where the binding of negatively charged PBDT molecule with  $\text{Ca}^{2+}$  ion creates ring  
 278 shaped concentric orientation pattern. According to our knowledge, it is the first success in  
 279 creating concentric ring pattern macroscopic superstructure in collagen hydrogel by diffusion  
 280 induced gelation. Attempt by Furusawa *et al.*<sup>22</sup> demonstrated that, diffusion of buffer through  
 281 the type I bovine dermis collagen solution made phase separated tubular pores aligned  
 282 parallel to the growth direction of the gel. This result suggests that different sources of  
 283 collagen have big impact for the creation of oriented structure. So we further performed  
 284 diffusion induced gelation in some traditionally used animal collagens as control experiment.  
 285 For this purpose, we used calf skin collagen (CSC) in tropocollagen form and porcine skin  
 286 collagen (PSC) in atelocollagen form. We found that both CSC and PSC only form very weak,

287 non-self-standing gels. Figure 5 shows the POM images of 2 wt% CSC and PSC samples  
 288 prepared at 25°C and 34°C. The samples prepared at 34°C are more turbid than that prepared  
 289 at 25°C (Figure 5), which indicates that these collagens have better fibrillogenesis capacity at  
 290 higher temperature. Interestingly, no birefringence is observed in all cases, except a thin weak  
 291 concentric birefringence at the periphery of PSC gel prepared at 34°C, indicating that almost  
 292 random structure is formed in both CSC and PSC hydrogel.



293  
 294  
 295 **Figure 5** The photographs (I) and POM images (II, III) of (a) 2 wt% calf skin collagen (CSC)  
 296 hydrogel and (b) 2 wt% porcine skin collagen (PSC) hydrogel prepared by 3 hours gelation at  
 297 25°C and 34°C. Illustrations (IV) of orientation patterns of collagen identified by POM are  
 298 shown on the right side of POM images. A: analyzer, P: polarizer, X' and Z': fast and slow  
 299 axes of the tint plate, respectively. All the images are in same scale as shown in the top left  
 300 part.  
 301

302 We have also confirmed orientation and morphology of fibril structure through SEM  
 303 observation. Figure 6 (a) and (b) show the SEM images of 4 wt% SBC solution and hydrogel,  
 304 respectively. All the samples were fixed by glutaraldehyde before performing SEM. SBC  
 305 solution does not contain any fibril, rather it makes cluster of network polymer (Figure 6(a)),  
 306 may be formed by glutaraldehyde crosslinking process. SBC hydrogel made by reaction-  
 307 diffusion (RD) process contains solely of collagen fibrils, which are beautifully aligned  
 308 perpendicular to the diffusion direction with an almost homogeneous fibril diameter of ~200  
 309 nm (Figure 6(b)). On the other hand, both CSC (Figure 6(c)) and PSC (Figure 6(d)) gels  
 310 contain randomly oriented collagen fibril with inhomogeneous distribution of fibril size.



311

312

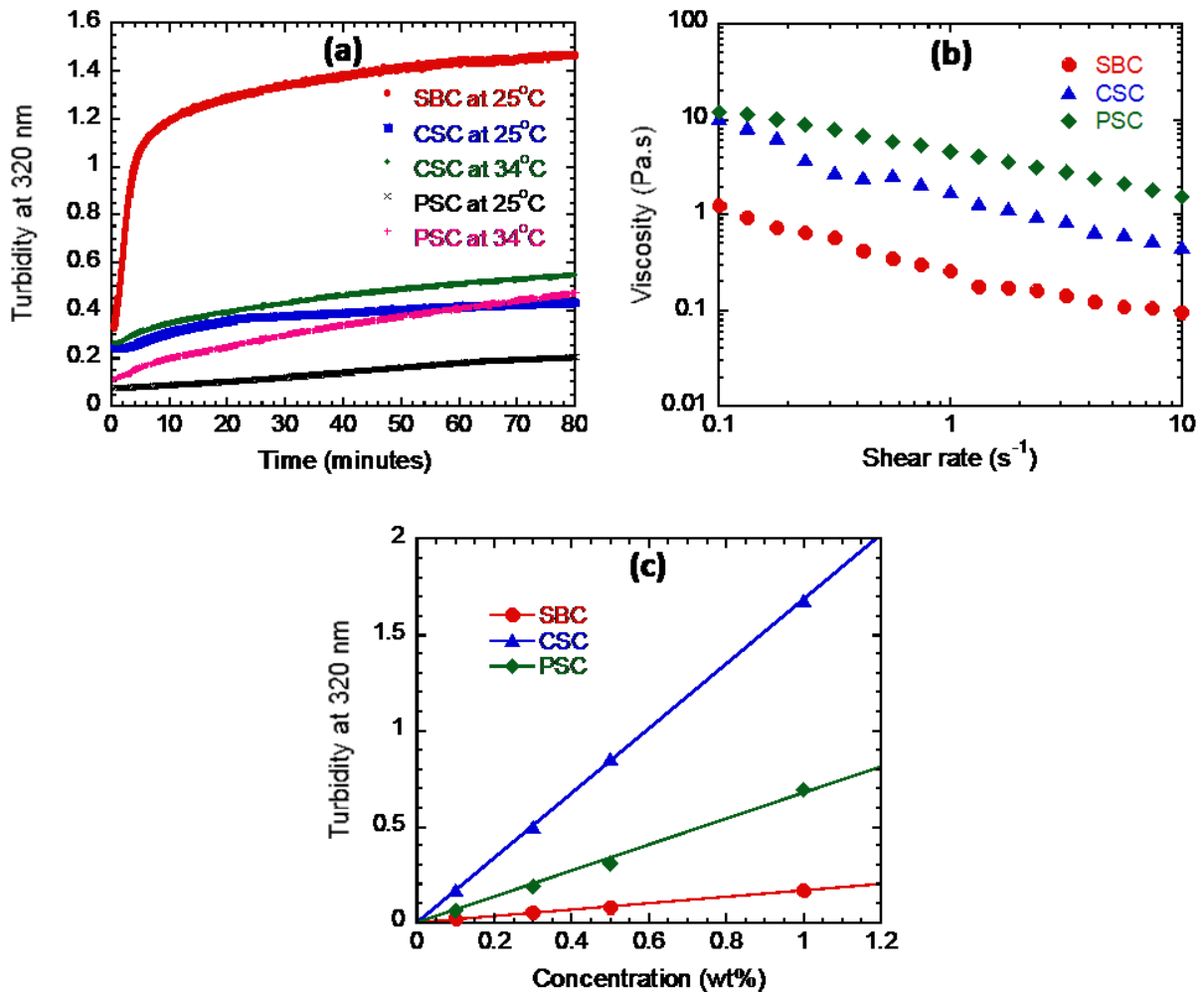
313 **Figure 6** SEM images of (a) 4 wt% SBC solution, (b) 4 wt% SBC gel prepared at 25°C, (c) 2  
 314 wt% CSC gel prepared at 34°C, (d) 2 wt% PSC gel prepared at 34°C. The red rectangular  
 315 markers in onset samples' photographs indicate the observation region of SEM images.  
 316 Lower row images are the magnified images of the corresponding upper row images.

317

318 One of the most important criteria we assumed, to develop internal stress from swelling  
 319 mismatch in the RD process, is the *fast rate of bundle formation* among the rigid  
 320 macromolecules with diffusing ions. Quick bundle formation causes large swelling mismatch



321 at the gel/sol phase boundary by solvent squeezing and therefore, can develop internal stress  
322 large enough to cause alignment of the rigid macromolecules along the gelation front line,  
323 which is frozen instantly to give the anisotropic structure. This may explain why, the  
324 fibrillogenesis rate of collagen in buffer solution must be very high to ensure the formation of  
325 aggregated structure by diffusion process and develop enough internal stress to create  
326 oriented structure. In the case of most of the conventional animal collagen, fibrillogenesis  
327 rate is very slow.<sup>17,43,44</sup> Zhang *et al.*<sup>17</sup> reported that, the fibrillogenesis rate of porcine tendon  
328 collagen is very slow compared to SBC. Figure 7(a) shows the comparative fibrillogenesis  
329 rate for SBC, CSC and PSC. At the present experimental conditions, fibrillogenesis rate of  
330 both animal collagens (CSC and PSC) is very slow, which ultimately causes the failure of  
331 creating oriented structure in CSC and PSC gels by diffusion induced gelation process.  
332 However, the fibrillogenesis rate of animal collagens (CSC and PSC) increases a bit at 34°C;  
333 but may be, still far away from the required quantity of gelation rate for the creation of  
334 ordered structure.



335

336 **Figure 7 (a)** Turbidity changes at 320 nm of an equal volume mixture of 0.3 wt% collagen  
 337 solution and 0.1 M Na-phosphate buffer (pH 7.2). The abrupt increase of turbidity of SBC  
 338 indicates its fast rate of *in vitro* fibril formation in the neutral buffer in comparison to CSC  
 339 and PSC. **(b)** The variation of dynamic viscosity (at 25°C) of acidic SBC, CSC and PSC  
 340 solutions with the shear rate ranges from 0.1 s<sup>-1</sup> to 10 s<sup>-1</sup>. **(c)** The concentration dependence of  
 341 turbidity at 320 nm (25°C) for acidic SBC, CSC and PSC solutions. The high turbidity of  
 342 CSC and PSC indicates the occurrence of fibril formation in comparison to SBC.

343

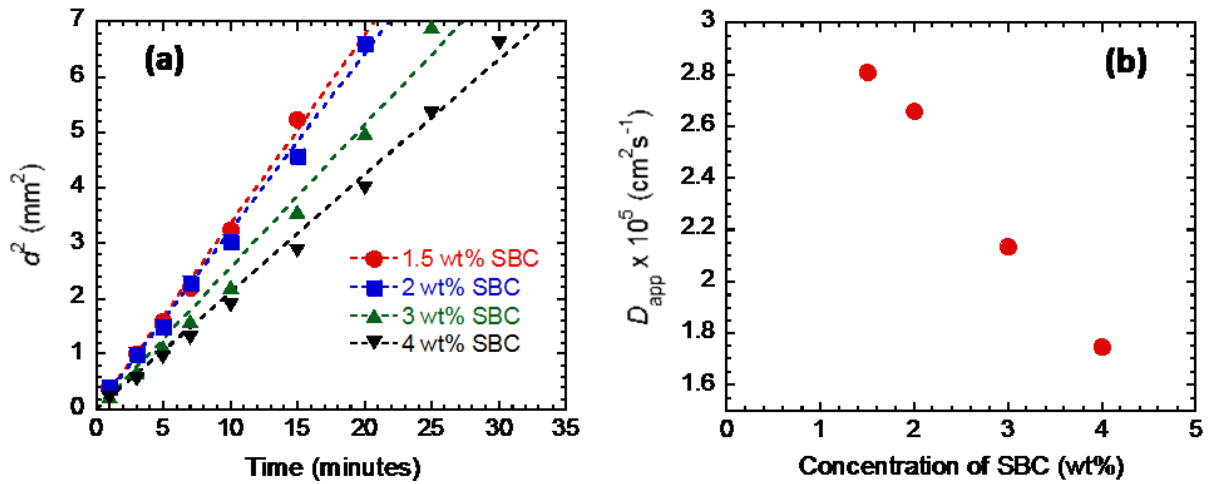
344 Additionally, the viscosity of animal collagens (CSC and PSC) in acidic solution increases  
 345 very rapidly with concentration, and above 2 wt% concentration, it becomes very difficult to  
 346 handle. For example, the viscosity of 1wt% CSC at 0.1 s<sup>-1</sup> is 10.14 Pa.s and 1wt% PSC is

347 12.05 Pa.s, which are about one order higher than that of SBC (1.25 Pa.s) (Figure 7(b)). The  
348 high viscosity of the CSC and PSC in acidic solution is due to the formation of aggregated  
349 structure, as shown by the dramatic increase of turbidity of animal collagens at high  
350 concentration (Figure 7(c)). We speculated that these aggregated structures make it difficult  
351 to form oriented structure of collagen by swelling mismatching. In contrast, SBC solution has  
352 much lower viscosity and turbidity than CSC and PSC. This makes it possible to perform the  
353 controlled gelation of SBC at high concentration (4 wt%), close to the native tissues. In  
354 summary, fast fibrillogenesis rate, high solubility and homogeneity, and low viscosity causes  
355 extremely high degree of fiber formation, which makes the SBC very special for forming  
356 hydrogels with ordered structure.

357

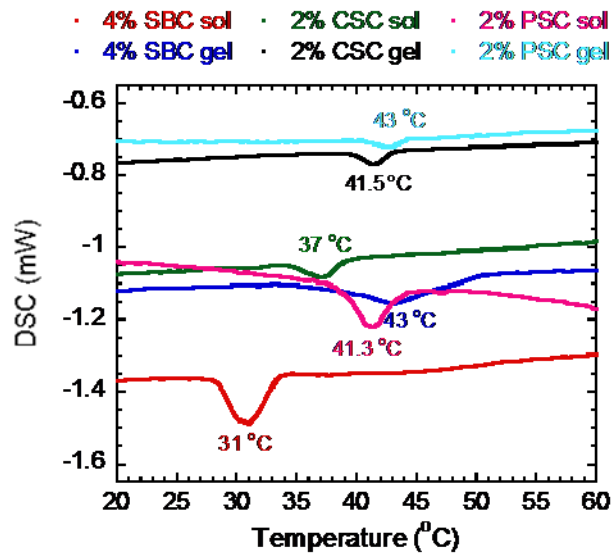
358 To get better understanding about the diffusion process, we quantitatively studied the  
359 diffusion features. The small ions of neutral phosphate buffer ( $\text{HPO}_4^{2-}$ ,  $\text{H}_2\text{PO}_4^-$ ,  $\text{Na}^+$ ) diffuse  
360 through the SBC solution and induce gelation. Since the fibrillogenesis rate of SBC is  
361 extremely fast and the translational motion of large triple-helix collagen molecule is very  
362 slow compared to the small buffer ions, it is expected that the gelation of SBC would be  
363 mostly controlled by the diffusion of buffer solution. This is confirmed by the linear  
364 relationship between the square of the gel layer width (distance between the periphery and the  
365 gelation front),  $d^2$  and the gelation time,  $t$  for different concentrations of SBC as shown in  
366 Figure 8(a). The apparent diffusion coefficient,  $D_{\text{app}}$  of 0.1 M Na-phosphate buffer (pH 7.2) is  
367 calculated from Figure 8(a) using the relationship,  $d^2 = 2D_{\text{app}}t^{45}$  and plotted against the  
368 concentrations of SBC in Figure 8(b). The values of  $D_{\text{app}}$  are in the same order with the  
369 diffusion constant of small ions in water ( $D_o(\text{HPO}_4^{2-}) = 1.49 \times 10^{-5} \text{ cm}^2\text{s}^{-1}$ ,  $D_o(\text{H}_2\text{PO}_4^-) = 1.03$   
370  $\times 10^{-5} \text{ cm}^2\text{s}^{-1}$ ,  $D_o(\text{Na}^+) = 2.53 \times 10^{-5} \text{ cm}^2\text{s}^{-1}$ ; calculated by using Stokes-Einstein equation<sup>46</sup>),  
371 and decrease linearly with increasing the concentrations of SBC. As the concentrations of

372 SBC increases, more buffer ions are consumed to induce fibrillogenesis and therefore, the  
 373  $D_{app}$  decreases.



374  
 375 **Figure 8 (a)** Relationship between the square of the gel layer width ( $d^2$ ) and gelation time ( $t$ )  
 376 for SBC hydrogels of various concentrations. **(b)** The change in apparent diffusion  
 377 coefficient,  $D_{app}$  (calculated from the slopes of (a) using the relationship,  $d^2 = 2D_{app}t$ ) of 0.1  
 378 M Na-phosphate buffer (pH 7.2) with the concentrations of SBC.

379  
 380 The differential scanning calorimetry (DSC) experiments (Figure 9) show that the  
 381 denaturation temperature ( $T_d$ ) of SBC hydrogel rises significantly from 31°C (32.9°C by CD  
 382 spectroscopy<sup>17</sup>) to 43°C after the gelation, indicating the formation of thick stable fiber by  
 383 diffusion induced gelation process. However in the case of CSC,  $T_d$  raises little from 37°C to  
 384 41°C, indicating that the further aggregation by buffer diffusion from the initial turbid  
 385 solution is not so high. Similar result was observed in PSC gel. Therefore, the samples  
 386 obtained from both CSC and PSC (at 25°C) was very weak and it broken into fragments when  
 387 we removed the cover glass of the reaction cell. On the contrary, SBC form strong gel that  
 388 could be handled easily.

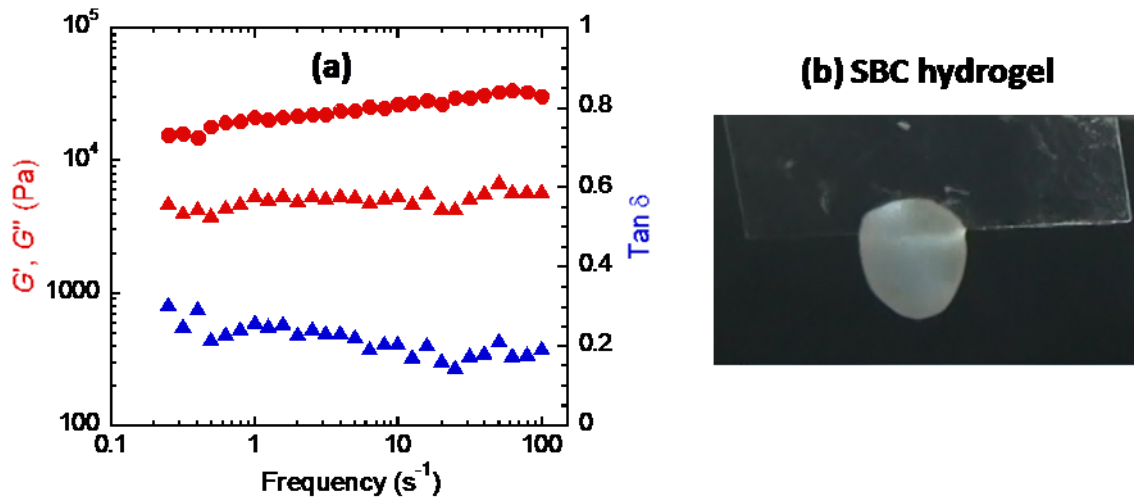


389

390 **Figure 9** DSC curves of SBC, CSC and PSC (both solution and hydrogel) heated at 1°C/min.

391

392 To characterize the mechanical strength of SBC hydrogel we have measured dynamic  
 393 modulus by applying torsion along the collagen orientation direction. The dynamic frequency  
 394 sweep test of 4 wt% SBC hydrogel at a constant strain of 0.2% is shown in Figure 10(a). The  
 395 SBC hydrogel shows a storage modulus about 15-30 kPa, which increases slightly with  
 396 frequency. The loss tangent is around 0.2. These results confirm that the SBC forms a soft  
 397 and elastic hydrogel. Figure 10(b) demonstrated that SBC gel can hang freely from the edge  
 398 of glass plate without any damage, indicating its self-standing ability. We found that the  
 399 mechanical strength and  $T_d$  value of SBC gel can be increased further by using chemical  
 400 cross-linker (data not shown). Since the strength of this 3D gel is sufficiently high and  $T_d$   
 401 value (43°C) is well above the physiological temperature, this material would be suitable for  
 402 cell culture and other biomedical applications.



403

404 **Figure 10 (a)** Frequency dependence of the storage modulus ( $G'$ - red circle), loss modulus  
 405 ( $G''$ - red triangle), and loss tangent ( $\tan \delta$ - blue triangle) of 4 wt% SBC gel at 25°C and a  
 406 constant strain amplitude of 0.2%. **(b)** Free hanging of 4 wt% SBC hydrogel from the edge of  
 407 glass without any damage indicates its self-standing ability.

408

#### 409 4. CONCLUSIONS

410 Disk shaped physical hydrogels with concentric orientation of collagen fibrils are prepared  
 411 from swim bladder collagen (SBC) of Bester sturgeon fish using a facile experimental  
 412 method. SBC meets all the criteria to form oriented and self-standing hydrogel by diffusion  
 413 induced gelation process. However, calf skin collagen (CSC) and porcine skin collagen (PSC)  
 414 could not form any oriented structure. The high aggregated structure, slow fibrillogenesis  
 415 rate, high viscosity and less homogeneity at high concentrations of animal collagens are not  
 416 favorable to form ordered structure by reaction-diffusion (RD) method. On the other hand,  
 417 the less aggregated structure, fast fibrillogenesis rate, and low viscosity of SBC solution favor  
 418 oriented superstructure formation by the controlled diffusion of buffer. Swelling mismatch  
 419 between the gel phase and the sol phase due to the quick solvent squeezing by fast  
 420 fibrillogenesis process (*syneresis effect*), generates an internal tensile stress in the collagen  
 421 molecules of gel phase, which assist them to align along the gel-sol interface direction to give

422 concentric ring-shaped orientation pattern. An anisotropic orientation gradient from periphery  
423 to center has been formed due to the change in diffusion velocity in respective regions. The  
424 denaturation temperature ( $T_d$ ) of SBC hydrogel rises significantly from 31°C of SBC solution  
425 to 43°C due to its excellent fiber forming capacity, however;  $T_d$  of both CSC and PSC gels  
426 increase a little from that of their solutions. SBC gel has reasonably high mechanical strength  
427 (storage modulus > 15 kPa). This SBC hydrogel made from marine-based atelocollagen,  
428 having macroscopic superstructure, self-standing capability and high thermal stability, will be  
429 suitable for cell culture and other biological applications. Our study would help to understand  
430 the mechanism and requirements for creating anisotropic hydrogel by RD method.  
431 Controlling the diffusion process of neutral buffer solution through SBC solution might be  
432 able to create different orientation pattern in SBC hydrogel, which offers further opportunity  
433 for functionalization of collagen hydrogel. SBC seems to have bright prospect for creating  
434 next generation artificial bio-materials.

435

## 436 **5. REFERENCES**

- 437 (1) J. P. Gong, Y. Katsuyama, T. Kurokawa and Y. Osada, *Adv. Mater.*, 2003, **15**, 1155-1158.
- 438 (2) M. A. Haque, G. Kamita, T. Kurokawa, K. Tsujii and J. P. Gong, *Adv. Mater.*, 2010, **22**,  
439 5110–5114.
- 440 (3) J. Y. Sun, X. Zhao, W. R. K. Illeperuma, O. Chaudhuri, K. H. Oh, D. j. Mooney, J. J.  
441 Vlassak and Z. Suo, *Nature*, 2012, **489**, 133–136.
- 442 (4) T. L. Sun, T. Kurokawa, S. Kuroda, A. B. Ihsan, T. Akasaki, K. Sato, M. A. Haque, T.  
443 Nakajima and J. P. Gong, *Nat. Mater.*, 2013, **12**, 932–937.
- 444 (5) R. Takahashi, Z. L. Wu, M. Arifuzzaman, T. Nonoyama, T. Nakajima, T. Kurokawa and  
445 J. P. Gong, *Nat. Commun.*, 2014, **5**, 4490.

- 446 (6) A. R. Liberski, J. T. Delaney, H. Schafer, J. Perelaer and U. S. Schubert, *Macromol.*  
447 *Biosci.*, 2011, **11**, 1491–1498.
- 448 (7) A. S. Hoffman, *Adv. Drug Delivery Rev.*, 2012, **64**, 18–23.
- 449 (8) B. V. Slaughter, S. S. Khurshid, O. Z. Fisher, A. Khademhosseini and N. A. Peppas, *Adv.*  
450 *Mater.*, 2009, **21**, 3307–3329.
- 451 (9) Y. Qiu and K. Park, *Adv. Drug Delivery Rev.*, 2012, **64**, 49–60.
- 452 (10) L. Cen, W. Liu, L. Cui, W. Zhang and Y. Cao, *Pediatr. Res.*, 2008, **63**, 492–496.
- 453 (11) R. Parenteau-Bareil, R. Gauvin and Berthod, F. *Materials*, 2010, **3**, 1863–1887.
- 454 (12) S. Weiner and H. D. Wagner, *Annu. Rev. Mater. Sci.*, 1998, **28**, 271–298.
- 455 (13) C. Sanchez, H. Arribart and M. M. Giraud-Guille, *Nat. Mater.*, 2005, **4**, 277–288.
- 456 (14) A. Jongjareonrak, S. Benjakul, W. Visessanguan, T. Nagai and M. Tanaka, *Food Chem.*,  
457 2005, **93**, 475–484.
- 458 (15) F. Zhang, A. Wang, Z. Li, S. He and L. Shao, *Food Nutr. Sci.*, 2011, **2**, 818–823.
- 459 (16) S. Yamada, K. Yamamoto, T. Ikeda, K. Yanagiguchi and Y. Hayashi, *BioMed Res. Int.*,  
460 2014, **2014**, 1–8.
- 461 (17) X. Zhang, M. Ookawa, Y. Tan, K. Ura, S. Adachi and Y. Takagi, *Food Chem.*, 2014,  
462 **160**, 305–312.
- 463 (18) T. Nagai and N. Suzuki, *Food Chem.*, 2000, **68**, 277–281.
- 464 (19) F. Pati, B. Adhikari and S. Dhara, *Bioresour. Technol.*, 2010, **101**, 3737–3742.
- 465 (20) A. Sanoa, M. Maedaa, S. Nagaharaa, T. Ochiyab, K. Honmac, H. Itohc, T. Miyatac and  
466 K. Fujiokaa, *Adv. Drug Delivery Rev.*, 2003, **55**, 1651–1677.
- 467 (21) W. Friess, *Eur. J. Pharm. Biopharm.*, 1998, **45**, 113–136.
- 468 (22) K. Furusawa, S. Sato, J. Masumoto, Y. Hanazaki, Y. Maki, T. Dobashi, T. Yamamoto,  
469 A. Fukui and N. Sasaki, *Biomacromolecules*, 2012, **13**, 29–39.
- 470 (23) N. Saeidi, E. A. Sander and J. W. Ruberti, *Biomaterials*, 2009, **30**, 6581–6592.



- 471 (24) P. Lee, R. Lin, J. Moon and L. P. Lee, *Biomed. Microdevices*, 2006, **8**, 35–41.
- 472 (25) F. Jiang, H. Horber, J. Howard and D. J. Muller, *J. Struct. Biol.*, 2004, **148**, 268–278.
- 473 (26) X. Cheng, U. A. Gurkan, C. J. Dehen, M. P. Tate, H. W. Hillhouse, G. J. Simpson and  
474 O. Akkus, *Biomaterials*, 2008, **29**, 3278–3288.
- 475 (27) J. A. Matthews, G. E. Wnek, D. G. Simpson and G. L. Bowlin, *Biomacromolecules*,  
476 2002, **3**, 232-238.
- 477 (28) C. Guo and L. J. Kaufman, *Biomaterials*, 2007, **28**, 1105–1114.
- 478 (29) J. Torbet, M. Malbouyres, N. Builles, V. Justin, M. Roulet, O. Damour, A. Oldberg, F.  
479 Ruggiero and Hulmes, D.J.S. *Biomaterials*, 2007, **28**, 4268–4276.
- 480 (30) R. M. Capito, H. S. Azevedo, Y. S. Velichko, A. Mata and S. I. Stupp, *Science*, 2008,  
481 **319**, 1812-1816.
- 482 (31) K. Furusawa, Y. Minamisawa, T. Dobashi and T. Yamamoto, *J. Phys. Chem. B*, 2007,  
483 **111**, 14423-14430.
- 484 (32) Y. Maki, K. Ito, N. Hosoya, C. Yoneyama, K. Furusawa, T. Yamamoto, T. Dobashi, Y.  
485 Sugimoto and K. Wakabayashi *Biomacromolecules*, 2011, **12**, 2145-2152.
- 486 (33) T. Dobashi, K. Furusawa, E. Kita, Y. Minamisawa and T. Yamamoto, *Langmuir*, 2007,  
487 **23**, 1303-1306.
- 488 (34) W. Yang, H. Furukawa and J. P. Gong, *Adv. Mater.*, 2008, **20**, 4499-4503.
- 489 (35) Z. L. Wu, T. Kurokawa, D. Sawada, J. Hu, H. Furukawa and J. P. Gong,  
490 *Macromolecules*, 2011, **44**, 3535-3541.
- 491 (36) Z. L. Wu, T. Kurokawa and J. P. Gong, *Polym. J.*, 2012, **44**, 503–511.
- 492 (37) Z. L. Wu, R. Takahashi, D. Sawada, M. Arifuzzaman, T. Nakajima, T. Kurokawa, J. Hu  
493 and J. P. Gong, *Macromolecules*, 2014, **47**, 7208–7214.
- 494 (38) J. A. Uquillas and O. Akkus, *Ann. Biomed. Eng.*, 2012, **40**, 1641-1653.

- 495 (39) Y. Li, A. Asadi, M. R. Monroe and E. P. Douglas, *Mater. Sci. Eng., C*, 2009, **29**, 1643-  
496 1649.
- 497 (40) M. M. Giraud-Guille, *Biol. Cell*, 1989, **67**, 97–101.
- 498 (41) F. Gobeaux, E. Belamie, G. Mosser, P. Davidson, P. Panine and M. M. Giraud-Guille,  
499 *Langmuir*, 2007, **23**, 6411-6417.
- 500 (42) M. Wolman and F.H. Kasten, *Histochemistry*, 1986, **85**, 41-49.
- 501 (43) B. R. Williams,; R. A. Gelman, D. C. Poppke and K. A. Piez, *J. Biol. Chem.*, 1978, **253**,  
502 6578-6585.
- 503 (44) G. C. Na, L. J. Butz and R. J. Carroll, *J. Biol. Chem.*, 1986, **261**, 12290-12299.
- 504 (45) A. Einstein, *Investigations on the Theory of Brownian Movement*; Dover: New York,  
505 1926.
- 506 (46) A. Einstein, *Annalen der Physik*, 1905, **17**, 549.
- 507
- 508
- 509
- 510
- 511
- 512
- 513
- 514
- 515
- 516
- 517
- 518
- 519

520 **Graphical abstract**

521

522 **Swim bladder collagen forms hydrogel with macroscopic superstructure by**  
523 **diffusion induced fast gelation**

524 Md. Tariful Islam Mredha<sup>a</sup>, Xi Zhang<sup>b</sup>, Takayuki Nonoyama<sup>c</sup>, Tasuku Nakajima<sup>c</sup>, Takayuki  
525 Kurokawa<sup>c</sup>, Yasuaki Takagi<sup>d</sup> and Jian Ping Gong<sup>c\*</sup>

526 <sup>a</sup>*Graduate School of Life Science, Hokkaido University, Sapporo 060-0810, Japan*

527 <sup>b</sup>*Graduate School of Fisheries Sciences, Hokkaido University, Hakodate 041-8611, Japan*

528 <sup>c</sup>*Faculty of Advanced Life Science, Hokkaido University, Sapporo 060-0810, Japan*

529 <sup>d</sup>*Faculty of Fisheries Sciences, Hokkaido University, Hakodate 041-8611, Japan*

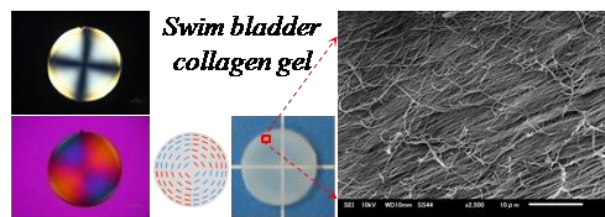
530 *\*Corresponding author-*

531 *E-mail: gong@mail.sci.hokudai.ac.jp (J.P.G); Tel & FAX: +81-(0)11-706-2774*

532

533

534



536

537

538 **Highlights**

539 Type I collagen extracted from swim bladder of Bester sturgeon forms oriented hydrogel with  
540 mechanical and thermal stability by diffusion induced fast gelation.